JOURNAL OF THE ROYAL SOCIETY Interface

J. R. Soc. Interface (2012) **9**, 988–996
doi:10.1098/rsif.2011.0462
Published online 14 September 2011

Cell wall structure and formation of maturing fibres of moso bamboo (*Phyllostachys pubescens*) increase buckling resistance

Xiaoqing Wang[1,*], Haiqing Ren[1], Bo Zhang[2,3], Benhua Fei[2] and Ingo Burgert[3,*]

[1]*Research Institute of Wood Industry, Chinese Academy of Forestry, Beijing, China*
[2]*Department of Biomaterials, International Centre for Bamboo and Rattan, Beijing, China*
[3]*Department of Biomaterials, Max Planck Institute of Colloids and Interfaces, Potsdam, Germany*

The mechanical stability of the culms of monocotyledonous bamboos is highly attributed to the proper embedding of the stiff fibre caps of the vascular bundles into the soft parenchymatous matrix. Owing to lack of a vascular cambium, bamboos show no secondary thickening growth that impedes geometrical adaptations to mechanical loads and increases the necessity of structural optimization at the material level. Here, we investigate the fine structure and mechanical properties of fibres within a maturing vascular bundle of moso bamboo, *Phyllostachys pubescens*, with a high spatial resolution. The fibre cell walls were found to show almost axially oriented cellulose fibrils, and the stiffness and hardness of the central part of the cell wall remained basically consistent for the fibres at different regions across the fibre cap. A stiffness gradient across the fibre cap is developed by differential cell wall thickening which affects tissue density and thereby axial tissue stiffness in the different regions of the cap. The almost axially oriented cellulose fibrils in the fibre walls maximize the longitudinal elastic modulus of the fibres and their lignification increases the transverse rigidity. This is interpreted as a structural and mechanical optimization that contributes to the high buckling resistance of the slender bamboo culms.

Keywords: *Phyllostachys pubescens*; micromechanics; cellulose fibrils; lignification; stiffness; buckling resistance

1. INTRODUCTION

Plants are able to adapt their material properties and organ geometry to cope with external and internal stresses they are subjected to [1]. The tissues of monocotyledonous bamboos are a highly eligible system to study such adaptations as cells stay alive and are modified during the entire plant development. This is because, unlike hardwood and softwood trees, bamboos develop only a primary shoot without secondary thickening growth which impedes geometrical adaptations and increases the necessity of structural optimization at the material level.

A cross section of the culm reveals inhomogeneous distribution of vascular bundles that are embedded in the parenchymatous ground tissue, densely dispersed in the outer and sparsely in the inner part of the culm wall (figure 1*a,b*). The vascular bundles mainly consisting of xylem, phloem and sclerenchymatous fibre caps or sheaths are the fundamental structural components of a bamboo culm, playing a decisive role in its physiological growth and biomechanical function (figure 1*c*). The conducting elements (vessels and phloem) provide a channel for the transport of water and nutrients, and the sclerenchymatous fibre caps primarily carry out the function of mechanical support. Therefore, the higher amount of vascular bundles in the outer culm wall is a perfect structural adaptation towards a high bending stiffness and strength of the bamboo culm.

The fibres, accounting for approximately 40 per cent of a culm by volume, are mainly distributed in the fibre caps surrounding the conducting elements. Within the developing fibre caps (immature), the fibres close to the vessels and the phloem finalize their wall thickening first, whereas those at the periphery of the fibre caps are in a transition state indicated by a large cell lumen. In these immature fibre caps, a pronounced density gradient can be observed from the inner fibres adjacent to the vessels towards the outer fibres connected to the surrounding parenchymatic tissue (figure 1*c*). Similar structural features have been examined for the fibre caps of a specific vascular bundle type of a palm tree (*Washingtonia robusta*) [2].

*Authors for correspondence (wangxq@caf.ac.cn; ingo.burgert@mpikg.mpg.de).

Received 13 July 2011
Accepted 22 August 2011

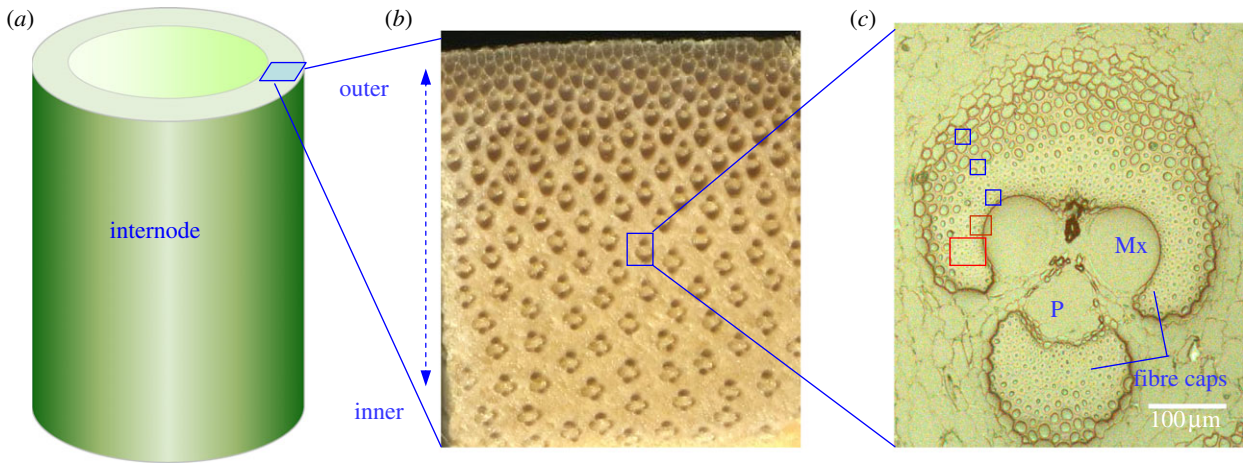

Figure 1. (*a*) Entire cross section of a two month-old culm of *Phyllostachys pubescens*. (*b*) Cross section of the culm wall showing the distribution of the vascular bundles. (*c*) Vascular bundle selected for nanoindentation (blue boxes) and Raman mapping (red boxes). Mx, metaxylem vessel; P, phloem.

The fibres are the main components determining the mechanical properties of bamboo owing to their unidirectional arrangement in the tissue as well as their unique cell wall structure [3,4]. In contrast to the sandwich-like structured secondary wall of wood fibres with a dominating middle layer (S1–S3), the bamboo fibres possess a much finer multi-layered wall structure with alternating broad and narrow sublayers [5,6]. An important ultrastructural feature of the wall is the variability in the orientation of the cellulose fibrils with respect to the longitudinal cell axis within different cell wall layers. The narrow layers possess a large microfibril angle indicating cellulose fibrils oriented almost perpendicular to the main cell axis, whereas the broad layers show a rather low microfibril angle which means that the cellulose fibrils are oriented basically parallel to the cell axis [5]. The degree of lignification varies remarkably across the fibre wall, with a higher lignin content present in the narrow layers. Besides the common matrix components of secondary walls (mainly hemicellulose and lignin), phenolic acids (e.g. ferulic and *p*-coumaric acids) are also widely distributed within the cell wall forming covalent linkage with lignin and polysaccharide components [7,8]. These specific features further contribute to the complexity of the design of the natural bamboo fibre wall.

Fibre wall anatomy [5,6], and in particular cell wall thickening [4,9], lignification [10,11] and cell wall nanostructural changes [12] during development of bamboo culms have been intensively studied. Only a few studies have been performed on mechanical properties of fibres or fibre caps [13–15], and the underlying structure–property relationships of bamboo fibres that establish the gradients across the fibre caps are not well understood yet.

To gain further insights into the mechanical performance of cell wall components and their interaction, it is necessary to probe the fine mechanical details within the cell wall and correlate them with the structural features of cell wall, such as microfibril angle and lignification. Nanoindentation allows for a close-up view on the mechanical properties of plant cell walls at the submicrometre level, and has been applied in a variety of studies on wood, bamboo and other cellulosic fibres [13,16,17]. By this technique, not only the mechanical properties of secondary wall layers, but also the mechanical variability within cell wall layers can be evaluated owing to the small indent size in the order of 100 nm [18]. In the present work, we used nanoindentation technique to investigate the cell wall mechanical properties of fibres within the vascular bundles of an immature bamboo culm in which cell wall thickening and lignification have not been finalized yet. In parallel, confocal Raman microscopy was used for imaging the chemical composition of the vascular bundles, and the cellulose and lignin distributions in different cell wall regions were visualized with high spatial resolution. In addition, the orientation of the cellulose molecules within the cell walls was examined by analysis of the cellulose-orientation-sensitive bands [19]. By combining the chemical and structural information derived from Raman mapping with the mechanical properties of fibres obtained by means of nanoindentation, we intended to gain insight into the mechanical design of bamboo fibre cell walls and shed light on the cell wall remodelling in vascular bundles during plant development.

2. MATERIAL AND METHODS

2.1. Plant material and preparation

A two month-old moso bamboo (*Phyllostachys pubescens*) culm was obtained from a local experimental forest in Miaoshanwu Nature Reserve of Zhejiang Province, China. The culm was 9.6 m in length with a diameter at breast height of 10 cm. Small sample blocks of approximately 15 mm (longitudinal) × 5 mm (tangential) × 5 mm (radial) were cut out of the 13th internode of the culm, and were immersed immediately in FAA (a mixture of formaldehyde, acetic acid and alcohol) for preserving the material. The sample blocks were stored in a refrigerator (5°C) prior to the chemical and mechanical testing. After being rinsed with distilled water, a sample block from the middle zone of the culm wall was selected and cut into two halves axially.

One half was used for Raman mapping, and the other for nanoindentation tests. This was done with the purpose of correlating the mechanical properties with the chemical information derived from the specific sample regions, which are the vascular bundles in the given case.

2.2. Raman mapping

The sample blocks for Raman mapping were embedded with water-soluble polyethylene glycol (PEG 2000). Specifically, the sample blocks were firstly dipped in a 1 : 1 solution of PEG and water at 60°C for 60 h, and were then kept in pure PEG at 60°C for 24 h prior to hardening by cooling down at room temperature. Approximately 6 µm-thick cross sections were cut from the embedded blocks using a rotary microtome (Leica RM2255, Germany). All sections were immediately transferred to glass slides and the water-soluble PEG was removed by repeated washing with distilled water. To avoid water evaporation during the measurement, the sections were sealed under cover slips with nail varnish. A confocal Raman microscope (CRM200, Witec, Germany) combined with a piezo scanner (P-500, Physik Instrumente, Germany) was used to collect the spectra. In order to achieve high spatial resolution, measurements were conducted with a microscope objective from Nikon (60×, NA = 0.8) and a linear polarized diode-pumped green laser (CrystaLaser, $\lambda = 532$ nm) with a diffraction-limited spot size of $0.61\lambda/\mathrm{NA}$. The Raman light was detected with a resolution of 6 cm^{-1} by an air-cooled, back-illuminated spectroscopic charge-coupled device (CCD) (ANDOR, USA) [20].

Measurement set-up and image processing were controlled with the software 'ScanCtrl Spectroscopy Plus' (Witec). For Raman spectroscopic mapping, an integration time of 1 s and a step size of 0.25 µm were chosen. Spectroscopic images were generated using a sum filter by integrating over defined wavenumber regions in the spectrum. Intensities were calculated within the selected borders and the background subtraction was performed by taking the baseline from the first to the second border. The areas selected for Raman scanning were marked by rectangles, including an inner region with metaxylem vessels and the surrounding fibres as well as a region further outward towards the periphery of the fibre cap (figure 1*c*). Cell wall regions of interest were marked for imaging the chemical composition and average spectra from these areas were calculated for detailed analysis.

2.3. Nanoindentation tests

Sample blocks for nanoindentation tests were dehydrated with ethanol and embedded in polymethylmethacrylate. The sample surfaces were prepared by grinding and polishing. Mechanical tests were performed with a nanoindenter (Hysitron Ubi1, USA), which was mounted on a vibration isolation table to minimize the disturbance of environmental vibrations. A three-sided pyramid diamond indenter tip (Berkovich type) with a radius of curvature of about 150 nm was used to image and indent the cell wall. The indenter tip was loaded in a force-controlled mode to a peak force of 180 µN at a rate of 36 $\mu\mathrm{N\,s}^{-1}$, then held at constant load for 6 s and further unloaded at a rate of 36 $\mu\mathrm{N\,s}^{-1}$. The longitudinal reduced elastic modulus (i.e. indentation modulus) and the hardness were calculated from the recorded load–displacement curves according to the method developed by Oliver & Pharr [21]. Three positions on the fibre cap with different distances to the vessel elements were probed—inner thick-walled fibres adjacent to the vessels, fibres in a transition region with thinner cell walls and larger lumina, and relatively thin-walled fibres in a region towards the periphery of the fibre cap. In order to create a profile of indentation modulus and hardness across the cell wall of fibres, a close-spaced indenting was adopted. Comparative studies with different spacing widths indicated that the load–displacement curves are only marginally affected by the indent density in bamboo fibre cell walls (data not shown). Fibres adjacent to the surrounding parenchyma were not selected for nanoindentation tests as their cell walls were regarded as being too thin for reliable indents. After indentation, an imaging scan of the fibre wall was performed by means of *in situ* scanning probe microscopy to evaluate the position and quality of indents. Owing to the embedding treatment, the nanoindentation experiments could not be conducted on native (wet) samples. However, all samples were treated equally which allows for comparing the mechanical properties on a relative basis.

3. RESULTS

3.1. Imaging the chemical composition of cell types

Pronounced differences were found in the Raman spectra of the different cell types, namely fibre, metaxylem vessel and parenchyma (figure 2*a*). The secondary cell wall of the fibres showed the most prominent lignin signals at 1597 and 1625 cm^{-1}, followed in turn by the parenchyma cells and the vessel. Further, the 2893 cm^{-1} band intensity was higher in the fibre walls compared with the other tissues, indicating a different cellulose orientation in the wall (see also figure 2*d*).

Two-dimensional spectroscopic images of the metaxylem vessel, the adjacent parenchyma cells and the surrounding fibres from the vascular bundle of *P. pubescens* were calculated by integrating over the intensity of defined Raman spectral bands (figure 2*b–d*). The overall structure of the measured cell walls can be visualized by integrating over the spectral range from 2789 to 3036 cm^{-1} involving C–H stretching vibrations present in carbohydrates and lignin [22,23]. The spectroscopic image clearly displayed higher intensity within the secondary cell wall of the thick-walled fibres, whereas the metaxylem vessel and the thin-walled parenchyma cells showed less intensity (figure 2*b*). The spatial distribution of lignin coupled with some phenolic acids (ferulic and *p*-coumaric acids) present in bamboo cell walls was visualized by integrating the intensity from 1517 to 1751 cm^{-1} (figure 2*c*). The secondary cell wall of fibres showed higher lignin signals than the metaxylem vessel and its adjacent parenchyma

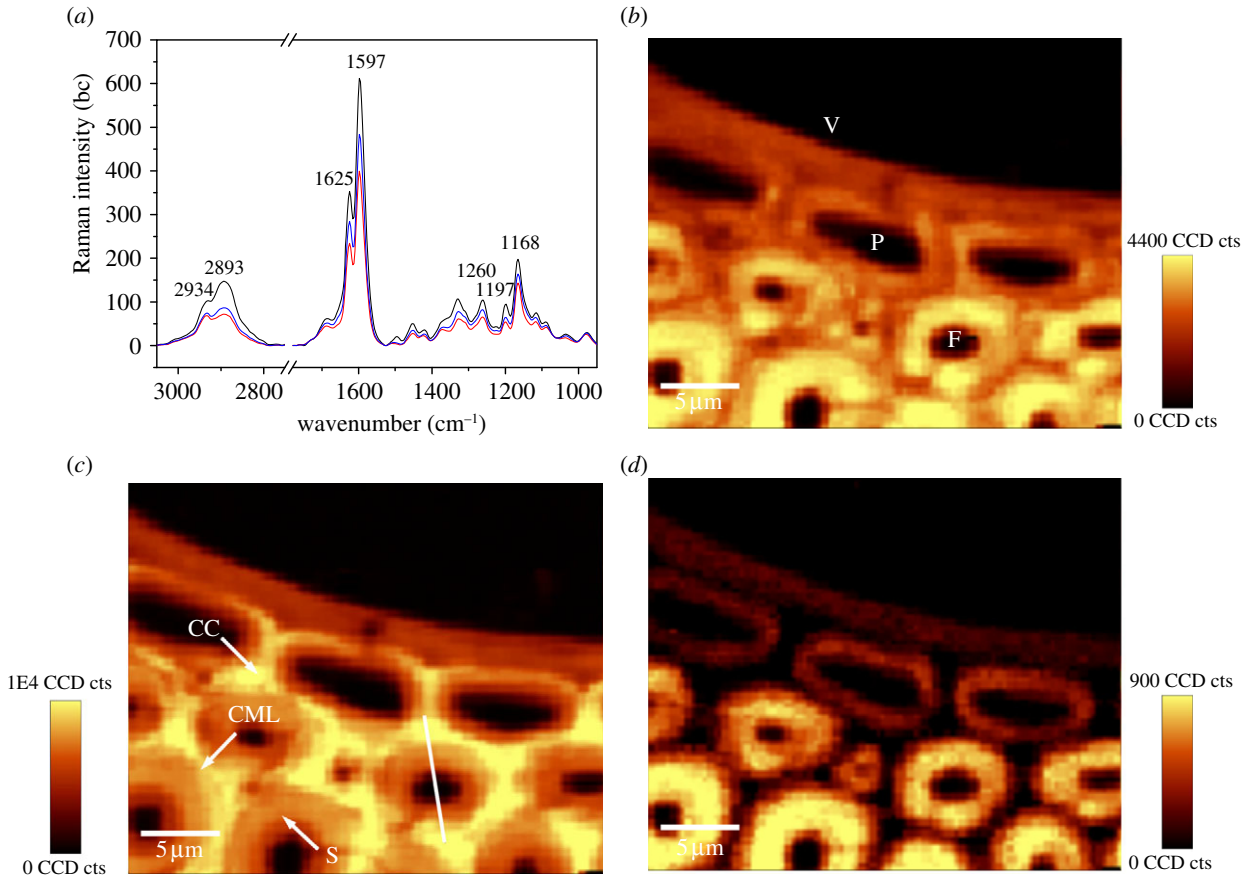

Figure 2. (*a*) Baseline corrected average Raman spectra of the secondary wall of the fibre (F, black line), metaxylem vessel (V, red line) and parenchyma cell (P, blue line) from the vascular bundle of *P. pubescens*. (*b*) Raman images of the metaxylem vessel (V), parenchyma cells (P) and the surrounding fibres (F) calculated by integrating from 2789 to 3036 cm^{-1} (all components). (*c*) Raman images integrating from 1517–1751 cm^{-1} (lignin coupled with phenolic acids). (*d*) 2793–2919 cm^{-1} (accentuating cellulose oriented in fibre direction).

cells. Integration over the strong band at 2893 cm^{-1} from 2793 to 2919 cm^{-1} emphasized the orientation-sensitive CH and CH_2 stretching of cellulose [20]. By this integration, the secondary cell wall of fibres displayed strong intensity indicating cellulose oriented basically in fibre direction, whereas the vessel and its adjacent parenchyma cells were visualized by weak signals (figure 2*d*).

Even within the individual cell wall of fibres, the lignin-associated compounds were distributed heterogeneously. The spectroscopic image shows cell corners (CCs) and compound middle lamella (CML) to be more lignified than the secondary cell walls of the fibres. To further visualize this gradient of lignification, Raman spectra were recorded from different positions (line marked in figure 2*c*) across the cell wall of a thick-walled fibre (figure 3*c*). The degree of lignification decreased from the outer to the inner layers across the cell wall as demonstrated by the band intensity profile. To gain further information, average Raman spectra were extracted from different cell wall layers (CC, CML, the secondary cell wall) of the fibres on the marked spectroscopic images (figure 3*a*,*b*). The Raman bands showed contributions from the major chemical components present in bamboo cell walls, such as cellulose, polyoses, lignin and phenolic acids. The most prominent bands were observed at 1597 and 1625 cm^{-1}, mainly derived from lignin and phenolic acids, and the next strongest band at 1168 cm^{-1} was primarily attributed to phenolic acids [23,24]. In the CC and CML spectra, a stronger fluorescence background was observed owing to the higher concentration of lignin and phenolic acids present (figure 3*a*). The CC of the fibres showed the most prominent lignin signals, followed in turn by the CML and the secondary cell wall (figure 3*b*).

The spectral region from 2789 to 3036 cm^{-1} is assigned to C–H stretching in lignin and carbohydrates [20]. Specifically, the peak at 2893 cm^{-1} attributed to C–H stretching of cellulose was more prominent in the spectrum of secondary cell wall, whereas in the CC and CML spectra the peak at 2934 cm^{-1} from the C–H stretching of the methoxyl groups of the lignin was more pronounced. The 1091 cm^{-1} band arises from symmetric and asymmetric stretching of C–O–C linkages of cellulose [25], which is highly sensitive to the orientation of cellulose, and seems to be more highlighted in the CC and CML spectra than in the spectrum of the secondary cell wall.

3.2. Imaging the chemical composition and nanomechanical probing of fibre cell walls

The second region of the vascular bundle (figure 1*c*, bigger red box) that was selected for Raman imaging allowed the

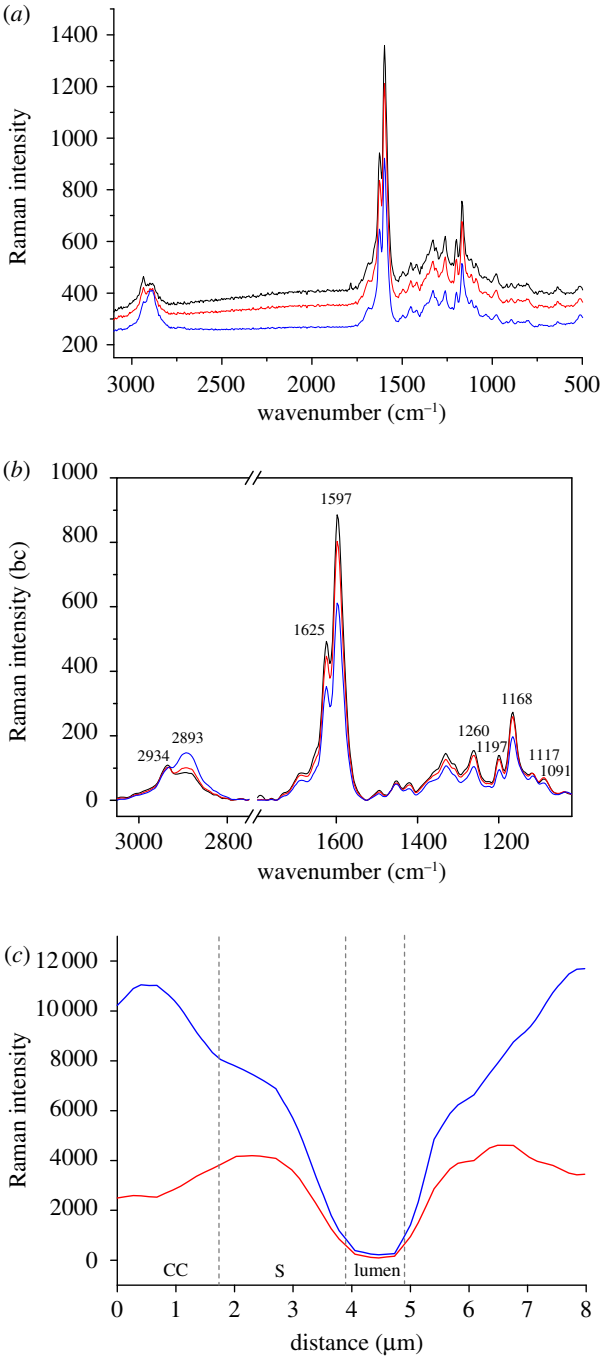

Figure 3. (*a*) Average Raman spectra of the cell corner (CC, black line), compound middle lamella (CML, red line) and the secondary wall of the fibre (S, blue line). (*b*) Baseline corrected (bc) spectra zoomed into the prominent bands. (*c*) Intensity distribution of lignin coupled with phenolic acids (1517–1751 cm^{-1}; blue curve) as well as all components (2789–3036 cm^{-1}; red curve) across the cell wall (line marked in figure 2*c*) of a thick-walled bamboo fibre.

structural and chemical features of fibre cell walls at different positions of the fibre cap to be studied. By integration of the region from 2807 to 3011 cm^{-1}, the basic morphology of the measured fibres became evident, characterized by thick-walled fibres close to the vessel (figure 4*a*, upper right corner) and thin-walled fibres in a more outside position (figure 4*a*, lower left corner).

Integration over the characteristic band of lignin and phenolic acids from 1527 to 1741 cm^{-1} showed remarkable heterogeneity in the distribution of these components within the cell wall of the fibres across the fibre cap (figure 4*b*). For the thick-walled fibres adjacent to the vessel, a higher degree of lignification was observed when compared with the thin-walled fibres outside, especially for the CC and CML regions. The CC and CML of the thin-walled fibres at the periphery were only poorly lignified.

By restricting the integration over the narrow bands at 2893 and 1091 cm^{-1} comprising information of cellulose orientation, the distribution of cellulose fibril orientation across the cell walls could be highlighted (figure 4*c*,*d*). Integration over the band at 2893 cm^{-1} revealed that the cellulose fibrils within the predominant secondary wall are aligned primarily parallel to the fibre axis (figure 4*c*). By integrating over the 1091 cm^{-1} band, the outmost layer (similar to the S1 layer in wood) of the secondary cell wall parallel to the electric field vector of the laser beam was visualized. In this case, the anticlockwise direction of the laser beam of an angle of approximately 45° highlighted the cellulose fibrils of this outer layer because of their orientation with a large angle to the fibre axis (figure 4*d*).

For the nanoindentation experiments, three regions of the fibre cap with different distances to the central vessel element were selected. The gradient-reversed images (figure 5*a*) show fibres with different cell wall thickness and lumen size related to their position in the fibre cap. Although being measured at a different position of the fibre cap, these characteristic fibre images fit well to the fibres observed by Raman imaging (figure 4). The images also denote the pattern of indents in the cell walls allowing the creation of a profile of indentation modulus and hardness of the cell wall from the lumen to the middle lamella (figure 5*b*).

The course of the indentation modulus from the lumen to the middle lamella showed the same trend for the three positions. Close to the lumen and close to the middle lamella the indentation modulus was lower than in the middle of the fibre cell wall. Between the inner and outer cell wall regions, the values reached a plateau with indentation moduli ranging around 18–20 GPa. Also in terms of hardness there was a great consistency in absolute values and trends across the fibre cell walls. The inner cell walls of fibres in all regions had a consistent hardness of approximately 400 MPa. A large variation of hardness values was observed for indents close to the lumen and the middle lamella, which is probably owing to the interference from the adjacent lumen and the middle lamella during the indentation process.

4. DISCUSSION

Vascular bundles are a fundamental structural component of the bamboo culm as they provide mechanical support and water–nutrient transport. To gain better understanding of the principles of mechanical optimization in vascular bundles, their underlying structure–property relationships have to be probed with high spatial resolution. In the present work, we investigated the chemical and mechanical properties

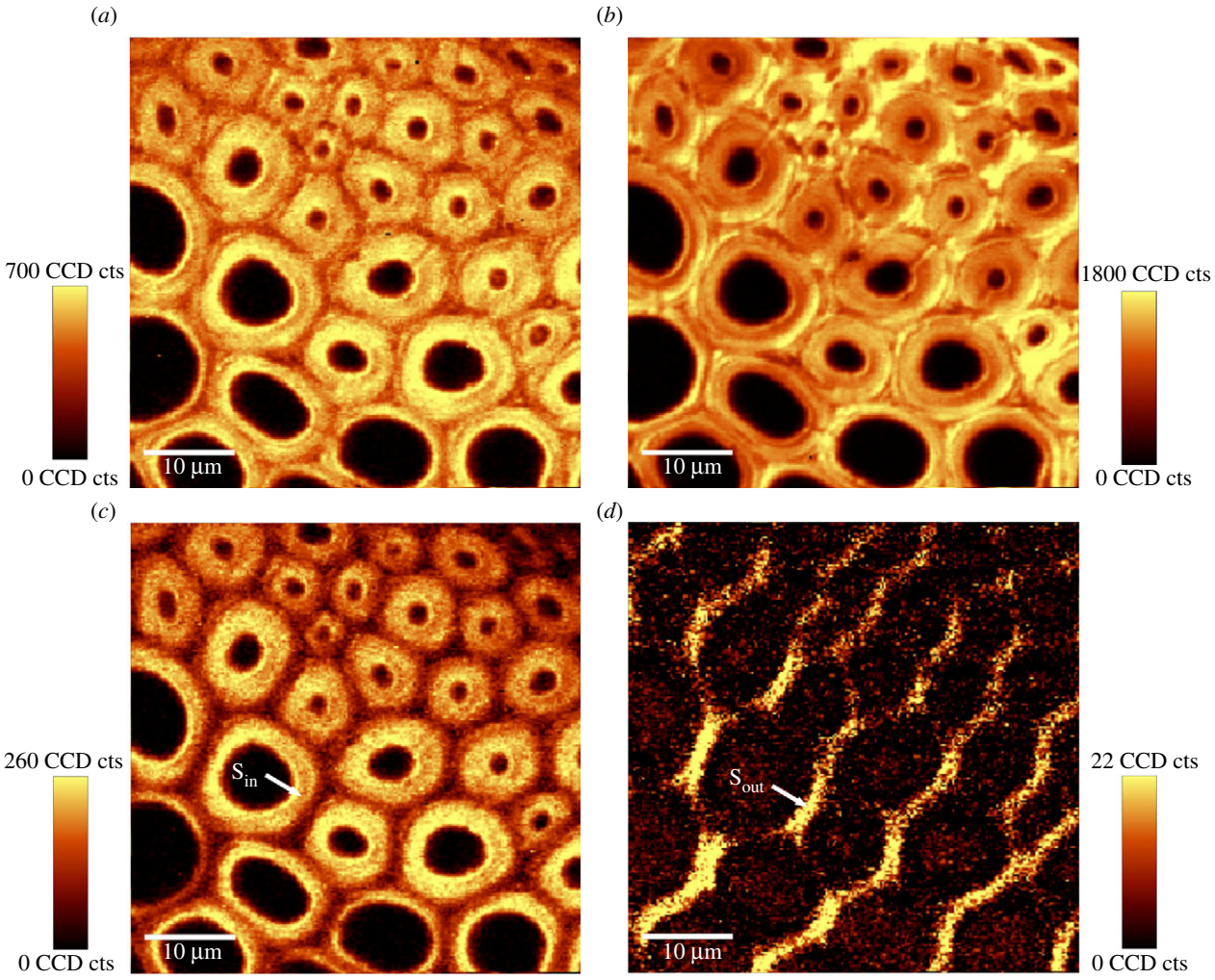

Figure 4. Raman images of the transition zone from thick-walled inner fibres to thin-walled outer fibres of the fibre cap of the vascular bundle (see also figure 1*c*). (*a*) Calculated by integrating from 2807 to 3011 cm^{-1} (all components), (*b*) 1527–1741 cm^{-1} (lignin coupled with phenolic acids), (*c*) 2819–2929 cm^{-1} (accentuating cellulose oriented in fibre direction), and (*d*) cellulose-orientation-sensitive band from 1069 to 1103 cm^{-1} (accentuating cell wall layers parallel to the electric field vector of the laser beam).

of a maturing fibre cap of moso bamboo *P. pubescens* by means of Raman mapping and nanoindentation. Confocal Raman microscopy with a spatial resolution of less than 1 µm was used to study the local distribution of lignin and cellulose in the present cell types and the different regions across the fibre cap (figure 2–4). The secondary wall of the fibres showed the highest level of lignification, followed by the parenchyma cells and the metaxylem vessel. A low lignin content in vessel walls was also reported for the bamboo *P. viridiglaucescens* based on a UV microspectrophotometry study [11]. This is contrary to the situation found in most deciduous trees in which the vessel walls are highly lignified to rigidify the wall [26], which is a necessity to cope with the large radial tensile forces resulting from the water transpiration stream. As it is reasonable to assume that the forces caused by the water transport are not lower in bamboo compared with deciduous trees, probably other mechanisms of vessel stabilization are used which are not yet understood.

In the cell walls of the fibres of the vascular bundles, the lignin-associated compounds were distributed heterogeneously (figure 2*c*). The CCs and the CMLs were heavily lignified, and the degree of lignification decreased from the outer layer to the inner layer of the fibre walls. This indicated that lignification was not fully completed, as the fibre walls were first lignified at the CC and CML. However, even within the CC, the lignin distribution seemed to be non-uniform (figure 3*c*). This variability in lignin concentration was also reported in the CC of black spruce wood (*Picea mariana*), which was attributed to the presence of non-lignified or poorly lignified regions in CC areas smaller than 1 µm [27].

The intensity of the lignin-associated bands at 1597 and 1625 cm^{-1} was very prominent compared with the cellulose bands in *P. pubescens* (figure 3) and was much stronger than the corresponding bands in wood [20,28]. This may be attributed to the unique lignin structure and composition in *P. pubescens*. It has been shown that bamboo lignin is composed of guaiacyl, syringyl and *p*-hydroxyphenylpropane units, which includes 5–10% of *p*-coumaric acid ester located at the γ-positions of the side chain of lignin [7,29]. Ferulic and *p*-coumaric acids are known to be linked with cell wall polysaccharides as well [8]. Raman spectroscopy

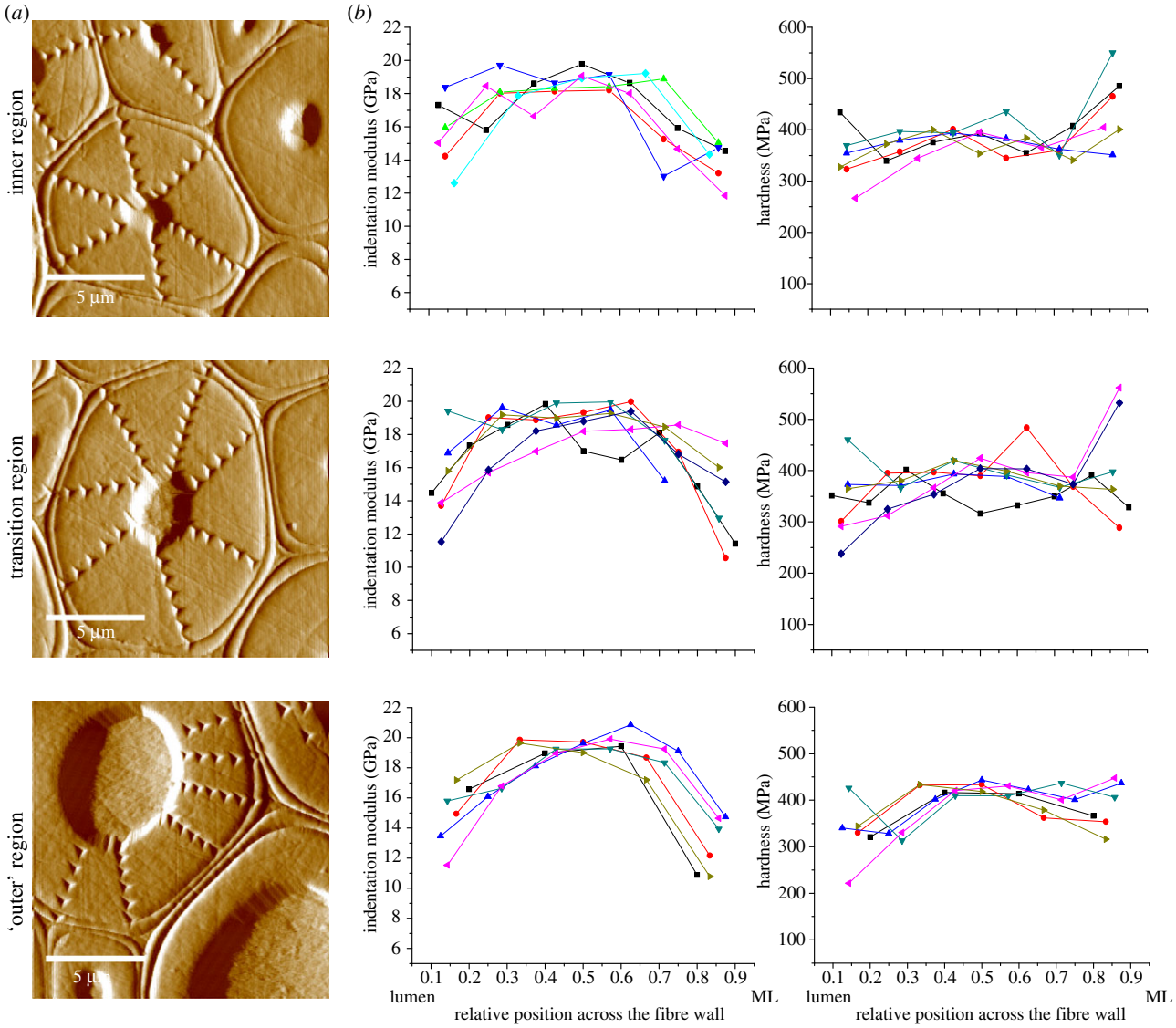

Figure 5. (*a*) Gradient reverse images of the fibre cell walls and indent patterns in the inner region, the transition region, and the 'outer' region of the fibre cap. (*b*) Indentation modulus and hardness of the cell walls measured from the lumen to the middle lamella (ML) for the fibres in the three aforementioned positions of the fibre cap. Owing to the irregular shape of the fibres, data points are shown according to their relative position between lumen (0) and middle lamella (1) on a normalized *x*-axis.

shows a high sensitivity in detecting aromatic ring-conjugated structures, which are present exactly in the ferulic and *p*-coumaric acids. As the spectral contributions of different lignin units are determined not only by their concentrations but also by pre-resonance Raman and conjugation effects [23], the strong bands at 1597 and 1625 cm^{-1} are supposed to be owing to both lignin and phenolic acids even though the latter is of low concentration in bamboo cell walls.

Fibres close to the vessel and phloem had already terminated cell wall thickening, whereas those at the periphery of the fibre cap were still in a developing stage indicated by thin cell walls (figure 1*c*). The lignification of a sequence of fibres covering different developmental stages from the centre to the periphery of the fibre cap was visualized by Raman mapping (figure 4*b*). The thick-walled fibres adjacent to the vessel showed a higher degree of lignification than those at the periphery of the fibre cap, especially in the CC and CML regions. The CC and CML of the thin-walled fibres at the periphery were only poorly lignified. This indicates a gradual transition in lignification across the maturing fibre cap which is consistent with other reports on cell wall lignification of bamboo [10,11,30].

The secondary wall of bamboo fibres is generally described as a polylamellate structure with alternating broad and narrow layers of different fibril orientation. The narrow layers are reported to show fibril angles of 85°–90° to the fibre axis and the broader ones have fibril angles almost parallel to the fibre axis [5,6]. The Raman spectra can provide information on the orientation of the cellulose molecules within the plant cell wall [19,31]. The spectral bands at 2893 and 1091 cm^{-1} are highly sensitive to the orientation of cellulose. Integration over the band at 2893 cm^{-1} revealed that cellulose fibrils of the secondary walls of fibres were oriented basically in fibre direction (figure 4*c*). Obviously,

the narrow layers could not be displayed owing to their limited widths (between 0.1 and 0.2 µm), which is below the geometric resolution of the scanning stage. Therefore, only the prominent broad layers were displayed giving an impression of a single layer (figure 4*c*). However, the outermost layer (similar to the S1 layer in wood) of the secondary walls of the fibres showed a rather large microfibril angle (figure 4*d*), which was also observed by Parameswaran & Liese [5], where fibrils are oriented at an angle of 50° with respect to the fibre axis.

The nanoindentation tests for measuring a profile of indentation modulus and hardness across the individual fibre cell walls were in good agreement with the Raman analysis of cellulose orientation (figure 5). The cell wall stiffness showed essentially the same trend from the lumen to the middle lamella for the fibres of the three positions, with higher stiffness in the middle and lower stiffness close to the lumen and middle lamella. Likewise, for the Raman mapping, it seems that the spatial resolution of the nanoindentation tests was too low to measure the mechanical properties of the alternating thin layers. The lower stiffness of the cell wall layers adjacent to the middle lamella can be either related to the larger microfibril angles or to interference by the close middle lamella. The lower stiffness of the inner cell wall region is likely to be an artefact, because of indenting close to the lumen of the fibre. It has been shown that the indentation modulus and hardness are highly dependent on both cellulose microfibril angle and lignin level of plant cell walls [16,32]. However, the degree of lignification seems to have a minor influence on the cell wall stiffness of bamboo fibres, which can be explained by the almost longitudinal orientation of the cellulose fibrils [33].

Owing to lack of a vascular cambium, arborescent monocotyledons show no secondary thickening growth that impedes geometrical adaptations to mechanical loads and increases the necessity of structural optimization at the material level. One crucial aspect for the mechanical stability of the trunk is the proper embedding of the stiff fibre caps of the vascular bundles into the soft parenchymatic matrix. In a previous study on a specific fibre cap type of the palm *W. robusta*, a gradual decrease in stiffness across the fibre cap was observed to avoid stress discontinuities between the stiffening elements and the soft parenchyma tissues, which was interpreted as an adaptation to the required mechanical constraints under the given growth conditions [2,34]. The stiffness gradient in the fibre cap of the palm is developed at two hierarchical levels: on the one hand at the tissue level owing to a decrease of tissue density (cell wall thickness/cell size) from the inner to the outer region, and on the other hand at the level of the cell wall assembly by regulating the level of lignin and its composition. In the case of the palm fibre cap, this affects the axial tensile stiffness, because the cell walls possess a high microfibril angle, and therefore the axial material properties of cell walls are highly dependent on the shear stiffness and strength of the matrix [35].

In terms of the investigated bamboo culm, the results do not indicate changes in cell wall properties across the fibre cap. The stiffness and hardness of the central part of the cell wall remain basically consistent for the fibres at the three positions across the fibre cap. As shown by the Raman imaging, the fibre cell walls of moso bamboo have almost axially oriented cellulose fibrils which impedes a regulation of axial tensile stiffness by the degree of lignification. Therefore, in the examined bamboo culm, a stiffness gradient across the fibre cap is mainly developed by differential cell wall thickening, which affects tissue density and thereby axial tissue stiffness of the different regions of the cap.

The different cell wall formation processes in palm and the bamboo might be explained by the different growth forms. Bamboo culms are much more slender than the palm trunks which make them more prone to buckling events. As they cannot increase the moment of inertia owing to a lack of secondary growth, the critical forces can only be shifted to high thresholds by maximizing the elastic modulus of the plant material. This requires that the fibre cell wall is as stiff as possible with almost axially oriented cellulose fibrils. Therefore, the stiffness gradient across the fibre cap in the immature state can only be achieved by thinner fibre walls at the periphery of the cap and a fine-tuning of cell wall properties seems to be infeasible.

The specific material optimization to reduce the buckling risk of the bamboo culm is mirrored by the interplay of cellulose and lignin in the cell assembly. As aforementioned, the orientation of cellulose fibril parallel to the cell axis makes the cell wall very stiff. Lignification does not further contribute to the stiffness but prevents cellulose fibrils from buckling under compressive loads by increasing the transverse rigidity.

Since only one specific type of vascular bundle from the middle zone of the culm wall of a specific internode was examined, the results may not generally be valid for the whole tissue or plant. However, our results indicate that the micro- and nanostructure of the investigated fibres is optimized towards to a high stiffness and buckling resistance. Thus, besides the hollow tube geometry, the structural and mechanical design of the fibre cell wall in terms of alternating cell wall layers as well as polymer orientation and composition is likely to contribute to the buckling resistance of the whole bamboo culm.

We thank Shumin Yang from the International Centre for Bamboo and Rattan (Beijing, China) for providing the bamboo samples and Annemarie Martins from the Max Planck Institute of Colloids and Interfaces (Potsdam, Germany) for embedding the samples for nanoindentation measurements. We are grateful for the help of Notburga Gierlinger from BOKU-University of Natural Resources and Applied Life Sciences (Vienna, Austria) for discussions regarding the Raman spectral data. This work was funded by the National Natural Science Foundation of China (nos. 30940056 and 30730076). We also acknowledge financial support from the International Centre for Bamboo and Rattan (no.1632009012).

REFERENCES

1 Niklas, K. J. 1992 *Plant biomechanics*. Chicago, IL: The University of Chicago Press.
2 Rüggeberg, M., Speck, T., Paris, O., Lapierre, C., Pollet, B., Koch, G. & Burgert, I. 2008 Stiffness gradients in vascular bundles of the palm *Washingtonia robusta*. *Proc. R. Soc. B* **275**, 2221–2229. (doi:10.1098/rspb.2008.0531)

3 Murphy, R. J. & Alvin, K. L. 1992 Variation in fibre wall structure in bamboo. *IAWA Bull. n. s.* **13**, 403–410.
4 Gritsch, C. S., Kleist, G. & Murphy, R. 2004 Developmental changes in cell wall structure of phloem fibres of the bamboo *Dendrocalamus asper*. *Ann. Bot.* **94**, 497–505. (doi:10.1093/aob/mch169)
5 Parameswaran, N. & Liese, W. 1976 On the fine structure of bamboo fibres. *Wood Sci. Technol.* **10**, 231–246. (doi:10.1007/BF00350830)
6 Parameswaran, N. & Liese, W. 1980 Ultrastructural aspects of bamboo cells. *Cell. Chem. Technol.* **14**, 587–609.
7 Higuchi, T. 1987 Chemistry and biochemistry of bamboo. *Bamboo J.* **4**, 132–145.
8 Ishii, T. & Hiroi, T. 1990 Linkage of phenolic acids to cell-wall polysaccharides of bamboo shoot. *Carbohydr. Res.* **206**, 297–310. (doi:10.1016/0008-6215(90)80069-F)
9 Murphy, R. J. & Alvin, K. L. 1997 Fibre maturation in the bamboo *Gigantochloa scortechinii*. *IAWA J.* **18**, 147–156.
10 Itoh, T. 1990 Lignification of bamboo (*Phyllostachys heterocycla* Mitf.) during its growth. *Holzforschung* **44**, 191–200. (doi:10.1515/hfsg.1990.44.3.191)
11 Lybeer, B. & Koch, G. 2005 A topochemical and semi-quantitative study of the lignification during ageing of bamboo culms (*Phyllostachys viridiglaucescens*). *IAWA J.* **26**, 99–109.
12 Suzuki, K. & Itoh, T. 2001 The changes in cell wall architecture during lignification of bamboo, *Phyllostachys aurea* Carr. *Trees* **15**, 137–147. (doi:10.1007/s004680000084)
13 Zou, L., Jin, H., Lu, W. Y. & Li, X. 2009 Nanoscale structural and mechanical characterization of the cell wall of bamboo fibers. *Mater. Sci. Eng. C* **29**, 1375–1379. (doi:10.1016/j.msec.2008.11.007)
14 Yu, Y., Jiang, Z., Fei, B., Wang, G. & Wang, H. 2011 An improved microtensile technique for mechanical characterization of short plant fibres: a case study on bamboo fibres. *J. Mater. Sci.* **46**, 739–746. (doi:10.1007/s10853-010-4806-8)
15 Yu, Y., Tian, G., Wang, H., Fei, B. & Wang, G. 2011 Mechanical characterization of single bamboo fibers with nanoindentation and microtensile technique. *Holzforschung* **65**, 113–119. (doi:10.1515/HF.2011.009)
16 Gindl, W., Gupta, H. S., Schöberl, T., Lichtenegger, H. C. & Fratzl, P. 2004 Mechanical properties of spruce wood cell walls by nanoindentation. *Appl. Phys. A* **79**, 2069–2073. (doi:10.1007/s00339-004-2864-y)
17 Wu, Y., Wang, S., Zhou, D., Xing, C., Zhang, Y. & Cai, Z. 2010 Evaluation of elastic modulus and hardness of crop stalks cell walls by nano-indentation. *Bioresour. Technol.* **101**, 2867–2871. (doi:10.1016/j.biortech.2009.10.074)
18 Konnerth, J., Gierlinger, N., Keckes, J. & Gindl, W. 2009 Actual versus apparent within cell wall variability of nanoindentation results from wood cell walls related to cellulose microfibril angle. *J. Mater. Sci.* **44**, 4399–4406. (doi:10.1007/s10853-009-3665-7)
19 Gierlinger, N. & Schwanninger, M. 2007 The potential of Raman microscopy and Raman imaging in plant research. *Spectroscopy* **21**, 69–89.
20 Gierlinger, N. & Schwanninger, M. 2006 Chemical imaging of poplar wood cell walls by confocal Raman microscopy. *Plant Physiol.* **140**, 1246–1254. (doi:10.1104/pp.105.066993)
21 Oliver, W. C. & Pharr, G. M. 1992 An improved technique for determining hardness and elastic modulus using load and displacement sensing indentation experiments. *J. Mater. Res.* **7**, 1564–1583. (doi:10.1557/JMR.1992.1564)
22 Agarwal, U. P. & Ralph, S. A. 1997 FT-Raman spectroscopy of wood: identifying contributions of lignin and carbohydrate polymers in the spectrum of black spruce (*Picea mariana*). *Appl. Spectrosc.* **51**, 1648–1655. (doi:10.1366/0003702971939316)
23 Agarwal, U. P. 1999 An overview of Raman spectroscopy as applied to lignocellulosic materials. In *Advances in lignocellulosics characterization* (ed. D. S. Argyropoulos), pp. 201–225. Atlanta, GA: TAPPI Press.
24 Takei, T., Kato, N., Iijima, T. & Higaki, M. 1995 Raman spectroscopic analysis of wood and bamboo lignin. *Mokuzai Gakkaishi* **41**, 229–236.
25 Edwards, H. G. M., Farwell, D. W. & Webster, D. 1997 FT Raman microscopy of untreated natural plant fibres. *Spectrochim. Acta A* **53**, 2383–2392. (doi:10.1016/S1386-1425(97)00178-9)
26 Donaldson, L. A. 2001 Lignification and lignin topochemistry—an ultrastructural view. *Phytochemistry* **57**, 859–873. (doi:10.1016/S0031-9422(01)00049-8)
27 Agarwal, U. P. 2006 Raman imaging to investigate ultrastructure and composition of plant cell walls: distribution of lignin and cellulose in black spruce wood (*Picea mariana*). *Planta* **224**, 1141–1153. (doi:10.1007/s00425-006-0295-z)
28 Lehringer, C., Gierlinger, N. & Koch, G. 2008 Topochemical investigation on tension wood fibres of Acer spp., *Fagus sylvatica* L. and *Quercus robur* L. *Holzforschung* **62**, 255–263. (doi:10.1515/HF.2008.036)
29 Fujii, Y., Azuma, J. & Okamura, K. 1996 Changes in chemical composition within an internode of elongating bamboo. *Holzforschung* **50**, 525–530. (doi:10.1515/hfsg.1996.50.6.525)
30 Lin, J., He, X., Hu, Y., Kuang, T. & Ceulemans, R. 2002 Lignification and lignin heterogeneity for various age classes of bamboo (*Phyllostachys pubescens*) stems. *Physiol. Plantarum* **114**, 296–302. (doi:10.1034/j.1399-3054.2002.1140216.x)
31 Gierlinger, N., Luss, S., Konig, C., Konnerth, J., Eder, M. & Fratzl, P. 2010 Cellulose microfibril orientation of *Picea abies* and its variability at the micron-level determined by Raman imaging. *J. Exp. Bot.* **61**, 587–595. (doi:10.1093/jxb/erp325)
32 Gindl, W., Gupta, H. S. & Grünwald, C. 2002 Lignification of spruce tracheid secondary cell walls related to longitudinal hardness and modulus of elasticity using nano-indentation. *Can. J. Bot.* **80**, 1029–1033. (doi:10.1139/B02-091)
33 Salmén, L. & Burgert, I. 2009 Cell wall features with regard to mechanical performance. *Holzforschung* **63**, 121–129. (doi:10.1515/HF.2009.011)
34 Rüggeberg, M., Speck, T. & Burgert, I. 2009 Structure-function relationships of different vascular bundle types in the stem of the Mexican Fanpalm (*Washingtonia robusta*). *New Phytol.* **182**, 443–450. (doi:10.1111/j.1469-8137.2008.02759.x)
35 Keckes, J. *et al.* 2003 Cell wall recovery after irreversible deformation of wood. *Nat. Mater.* **2**, 810–814. (doi:10.1038/nmat1019)